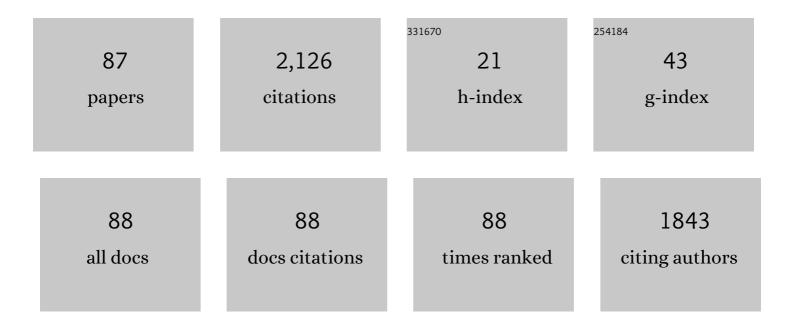
## Hou-Bing Huang

List of Publications by Year in descending order

Source: https://exaly.com/author-pdf/6226792/publications.pdf Version: 2024-02-01



#	Article	IF	CITATIONS
1	Ultrahigh energy storage in superparaelectric relaxor ferroelectrics. Science, 2021, 374, 100-104.	12.6	276
2	Super-elastic ferroelectric single-crystal membrane with continuous electric dipole rotation. Science, 2019, 366, 475-479.	12.6	272
3	High-entropy enhanced capacitive energy storage. Nature Materials, 2022, 21, 1074-1080.	27.5	161
4	High-entropy polymer produces a giant electrocaloric effect at low fields. Nature, 2021, 600, 664-669.	27.8	121
5	Toward Wearable Cooling Devices: Highly Flexible Electrocaloric Ba <sub>0.67</sub> Sr <sub>0.33</sub> TiO <sub>3</sub> Nanowire Arrays. Advanced Materials, 2016, 28, 4811-4816.	21.0	101
6	Role of Reversible Phase Transformation for Strong Piezoelectric Performance at the Morphotropic Phase Boundary. Physical Review Letters, 2018, 120, 055501.	7.8	84
7	Water printing of ferroelectric polarization. Nature Communications, 2018, 9, 3809.	12.8	75
8	Toroidal polar topology in strained ferroelectric polymer. Science, 2021, 371, 1050-1056.	12.6	74
9	Hybrid Magnetic Micropillar Arrays for Programmable Actuation. Advanced Materials, 2020, 32, e2001879.	21.0	58
10	Size-Dependent Phase Transition in Perovskite Nanocrystals. Journal of Physical Chemistry Letters, 2019, 10, 5451-5457.	4.6	48
11	Simultaneously achieving giant piezoelectricity and record coercive field enhancement in relaxor-based ferroelectric crystals. Nature Communications, 2022, 13, 2444.	12.8	46
12	Size effects of electrocaloric cooling in ferroelectric nanowires. Journal of the American Ceramic Society, 2018, 101, 1566-1575.	3.8	38
13	Ferroelectric domain-wall logic units. Nature Communications, 2022, 13, .	12.8	37
14	How Far Can We Push the Rigid Oligomers/Polymers toward Ferroelectric Nematic Liquid Crystals?. Journal of the American Chemical Society, 2021, 143, 17857-17861.	13.7	36
15	Defectâ€Engineered Dzyaloshinskii–Moriya Interaction and Electricâ€Fieldâ€Switchable Topological Spin Texture in SrRuO <sub>3</sub> . Advanced Materials, 2021, 33, e2102525.	21.0	34
16	Improper molecular ferroelectrics with simultaneous ultrahigh pyroelectricity and figures of merit. Science Advances, 2021, 7, .	10.3	32
17	High electrocaloric effect in hotâ€pressed Pb <sub>0.85</sub> La <sub>0.1</sub> (Zr <sub>0.65</sub> Ti <sub>0.35</sub> )O <sub>3</sub> ceramics with a wide operating temperature range. Journal of the American Ceramic Society, 2017, 100, 4581-4589.	3.8	30
18	Core–Shell Magnetic Micropillars for Reprogrammable Actuation. ACS Nano, 2021, 15, 4747-4758.	14.6	30

#	Article	IF	CITATIONS
19	Magnetically actuated functional gradient nanocomposites for strong and ultra-durable biomimetic interfaces/surfaces. Materials Horizons, 2017, 4, 869-877.	12.2	28
20	Designed Giant Roomâ€Temperature Electrocaloric Effects in Metalâ€Free Organic Perovskite [MDABCO](NH <sub>4</sub> )I <sub>3</sub> by Phase–Field Simulations. Advanced Functional Materials, 2021, 31, 2104393.	14.9	27
21	The strong electrocaloric effect in molecular ferroelectric ImClO <sub>4</sub> with ultrahigh electrocaloric strength. Journal of Materials Chemistry A, 2020, 8, 16189-16194.	10.3	23
22	Phase-field simulations of vortex chirality manipulation in ferroelectric thin films. Npj Quantum Materials, 2022, 7, .	5.2	22
23	Large Room Temperature Negative Electrocaloric Effect in Novel Antiferroelectric PbHfO <sub>3</sub> Films. ACS Applied Materials & Interfaces, 2021, 13, 21331-21337.	8.0	21
24	Influences of grain/particle interfacial energies on second-phase particle pinning grain coarsening of polycrystalline. Journal of Alloys and Compounds, 2020, 818, 152848.	5.5	19
25	Analysis of multi-domain ferroelectric switching in BiFeO3 thin film using phase-field method. Computational Materials Science, 2016, 115, 208-213.	3.0	18
26	Grain boundary curvature based 2D cellular automata simulation of grain coarsening. Journal of Alloys and Compounds, 2019, 791, 411-422.	5.5	18
27	Understanding and predicting geometrical constraint ferroelectric charged domain walls in a BiFeO3 island via phase-field simulations. Applied Physics Letters, 2018, 113, .	3.3	17
28	Understanding electrocaloric cooling of ferroelectrics guided by phaseâ€field modeling. Journal of the American Ceramic Society, 2022, 105, 3689-3714.	3.8	17
29	Phase-field simulations of surface charge-induced polarization switching. Applied Physics Letters, 2019, 114, .	3.3	15
30	Phase-field simulation of multi-phase interactions in Fe-C peritectic solidification. Computational Materials Science, 2020, 171, 109220.	3.0	15
31	Domain evolution in bended freestanding BaTiO3 ultrathin films: A phase-field simulation. Applied Physics Letters, 2020, 116, .	3.3	15
32	Nanoscale Bandgap Tuning across an Inhomogeneous Ferroelectric Interface. ACS Applied Materials & Interfaces, 2017, 9, 24704-24710.	8.0	14
33	Bioinspired Wearâ€Resistant and Ultradurable Functional Gradient Coatings. Small, 2018, 14, e1802717.	10.0	14
34	Switching the chirality of a magnetic vortex deterministically with an electric field. Materials Research Letters, 2018, 6, 669-675.	8.7	13
35	Strain Engineering of Energy Storage Performance in Relaxor Ferroelectric Thin Film Capacitors. Advanced Theory and Simulations, 2022, 5, .	2.8	13
36	Strain-induced broadening temperature range of electrocaloric effects in ferroelectric superlattices. Journal of Alloys and Compounds, 2019, 777, 821-827.	5.5	12

#	Article	IF	CITATIONS
37	Ferroelasticâ€Domainâ€Assisted Mechanical Switching of Ferroelectric Domains in Pb(Zr,Ti)O <sub>3</sub> Thin Films. Advanced Electronic Materials, 2020, 6, 2000300.	5.1	12
38	Phase-field model of graphene aerogel formation by ice template method. Applied Physics Letters, 2019, 115, 111901.	3.3	11
39	Selfâ€Assembled Epitaxial Ferroelectric Oxide Nanospring with Super‣calability. Advanced Materials, 2022, 34, e2108419.	21.0	11
40	Tip-Induced In-Plane Ferroelectric Superstructure in Zigzag-Wrinkled BaTiO <sub>3</sub> Thin Films. Nano Letters, 2022, 22, 2859-2866.	9.1	11
41	Thickness Dependence of Switching Behavior in Ferroelectric BiFeO3 Thin Films: A Phase-Field Simulation. Applied Sciences (Switzerland), 2017, 7, 1162.	2.5	10
42	Wide Electrocaloric Temperature Range Induced by Ferroelectric to Antiferroelectric Phase Transition. Applied Sciences (Switzerland), 2019, 9, 1672.	2.5	10
43	Ultrafast Ferroelectric Domain Switching Induced by Nanoâ€Second Strainâ€Pulse. Advanced Theory and Simulations, 2022, 5, .	2.8	10
44	Phase-field simulations of surface charge-induced ferroelectric vortex. Journal Physics D: Applied Physics, 2021, 54, 405302.	2.8	9
45	Magnetization switching modes in nanopillar spin valve under the external field. Science China: Physics, Mechanics and Astronomy, 2011, 54, 1227-1234.	5.1	8
46	Numerical simulation of vortex dynamics in type-II superconductors in oscillating magnetic field using time-dependent Ginzburg–Landau equations. Journal of Physics Condensed Matter, 2017, 29, 505701.	1.8	8
47	Multiphase-field approach with parabolic approximation scheme. Computational Materials Science, 2020, 172, 109322.	3.0	8
48	Fe-C peritectic solidification of polycrystalline ferrite by phase-field method. Computational Materials Science, 2020, 178, 109626.	3.0	8
49	Investigation into electrocaloric effect of different types of ferroelectric materials by Landau-Devonshire theory. Wuli Xuebao/Acta Physica Sinica, 2020, 69, 217801.	0.5	8
50	Electric-Field-Insensitive Temperature Stability of Strain in KNN Multilayer Composite Ceramics. ACS Applied Materials & Interfaces, 2022, 14, 26949-26957.	8.0	8
51	Numerical Simulation of Phase Transitions in Type-II Annular Superconductor Using Time-dependent Ginzburg-Landau Equations. Journal of Superconductivity and Novel Magnetism, 2018, 31, 3445-3451.	1.8	7
52	Polarization-switching pathway determined electrical transport behaviors in rhombohedral BiFeO <sub>3</sub> thin films. Nanoscale, 2021, 13, 17746-17753.	5.6	7
53	Antiferroelectric Phase Diagram Enhancing Energy-Storage Performance by Phase-Field Simulations. ACS Applied Materials & Interfaces, 2022, 14, 25770-25780.	8.0	7
54	Determining dendrite arm spacing in directional solidification using a fast Fourier transform method. Computational Materials Science, 2020, 173, 109463.	3.0	6

#	Article	IF	CITATIONS
55	Phase Diagram of Subâ€GHz Electricâ€Fieldâ€Induced Polarization Oscillation. Physica Status Solidi - Rapid Research Letters, 2022, 16, 2100416.	2.4	6
56	Microscopic physical origin of polarization induced large tunneling electroresistance in tetragonal-phase BiFeO3. Acta Materialia, 2022, 225, 117564.	7.9	6
57	Strain manipulation of ferroelectric skyrmion bubbles in a freestanding <mml:math xmlns:mml="http://www.w3.org/1998/Math/MathML"&gt;<mml:msub><mml:mi>PbTiO</mml:mi><mml:mn>3film: A phase field simulation. Physical Review B, 2022, 105, .</mml:mn></mml:msub></mml:math 	ml:man2> <td>mm<b>k</b>msub&gt;&lt;</td>	mm <b>k</b> msub><
58	Multi-scale simulations of metamagnetic martensite transition in NiCoMnIn. Journal of Alloys and Compounds, 2016, 689, 507-511.	5.5	5
59	Current assisted memory effect in superconductor–ferromagnet bilayers: a potential candidate for memristors. Superconductor Science and Technology, 2019, 32, 095002.	3.5	5
60	Influences of particle fractions on second-phase particles pinning grain coarsening processes. Journal of Materials Science, 2020, 55, 3434-3449.	3.7	5
61	Quantitative investigation of polar nanoregion size effects in relaxor ferroelectrics. Acta Materialia, 2022, 237, 118147.	7.9	5
62	Micromagnetic simulation of electric field-modulation on precession dynamics of spin torque nano-oscillator. Applied Physics Letters, 2017, 111, .	3.3	4
63	Tunable temperature dependence of electric-field-control multicaloric effects. Journal of Alloys and Compounds, 2019, 806, 1491-1496.	5.5	4
64	Explicit Dynamics of Diffuse Interface in Phaseâ€Field Model. Advanced Theory and Simulations, 2021, 4, .	2.8	4
65	Visualization of large-scale charged domain Walls in hexagonal manganites. Applied Physics Letters, 2021, 118, .	3.3	4
66	Phase field simulation of misfit strain manipulating domain structure and ferroelectric properties in PbZr <sub>(1–<i>x</i>)</sub> Ti <i><sub>x</sub></i> O <sub>3</sub> thin films. Wuli Xuebao/Acta Physica Sinica, 2020, 69, 127801.	0.5	4
67	Designing Ultrafast Cooling Rate for Room Temperature Electrocaloric Effects by Phaseâ€Field Simulations. Advanced Theory and Simulations, 2022, 5, .	2.8	4
68	Simulation of stress-modulated magnetization precession frequency in Heusler-based spin torque oscillator. Journal of Magnetism and Magnetic Materials, 2017, 426, 415-420.	2.3	3
69	Hydride corrosion kinetics on metallic surface: a multiphase-field modeling. Materials Research Express, 2021, 8, 106518.	1.6	3
70	Photoenhanced Electroresistance at Dislocation-Mediated Phase Boundary. ACS Applied Materials & Interfaces, 2022, 14, 18662-18670.	8.0	3
71	Phase-Field Model of Hydride Blister Growth Kinetics on Zirconium Surface. Frontiers in Materials, 2022, 9, .	2.4	3
72	Micromagnetic Simulation of Strain-Assisted Current-Induced Magnetization Switching. Advances in Condensed Matter Physics, 2016, 2016, 1-6.	1.1	2

#	Article	IF	CITATIONS
73	Simulation of Magnetically-Actuated Functional Gradient Nanocomposites. Applied Sciences (Switzerland), 2017, 7, 1171.	2.5	2
74	Phase-field simulation of two-dimensional topological charges in nematic liquid crystals. Journal of Applied Physics, 2020, 128, 124701.	2.5	2
75	Domain wall tuned superconductivity in superconductor–ferromagnet bilayers. Journal Physics D: Applied Physics, 2020, 53, 375001.	2.8	2
76	Multi-phase-field simulation of austenite peritectic solidification based on a ferrite grain*. Chinese Physics B, 2021, 30, 018201.	1.4	2
77	Phase-Field Simulation of Superconductor-Ferromagnet Bilayer-Based Cryogenic Strain Sensor. Journal of Superconductivity and Novel Magnetism, 2022, 35, 409-414.	1.8	2
78	Pressure-induced room temperature electrocaloric effect in BiFeO3-PbTiO3 solid solution based on Landau-Devonshire theory. Materials Today Communications, 2022, 31, 103396.	1.9	2
79	Boundary Pinning Effects on the Frequency Spectra of Point-Contact Spin-Torque Oscillators. IEEE Magnetics Letters, 2018, 9, 1-4.	1.1	1
80	Theoretically optimized hybrid magnetic nanoparticle concentrations for functional gradient nanocomposites. AIP Advances, 2020, 10, 105209.	1.3	1
81	Defectâ€Engineered Dzyaloshinskii–Moriya Interaction and Electricâ€Fieldâ€Switchable Topological Spin Texture in SrRuO <sub>3</sub> (Adv. Mater. 33/2021). Advanced Materials, 2021, 33, 2170255.	21.0	1
82	Enhancing the Elastocaloric Strength by Combining Positive and Negative Elastocaloric Effects. Physica Status Solidi - Rapid Research Letters, 2022, 16, .	2.4	1
83	Effect of Background Magnetic Field on Type-II Superconductor under Oscillating Magnetic Field Simulated Using Ginzburg-Landau Model. Advances in Condensed Matter Physics, 2018, 2018, 1-7.	1.1	0
84	Phase-field model of topological charge interaction force in nematic liquid crystals. Soft Materials, 2020, , 1-6.	1.7	0
85	A parabolic approximation scheme for multi-phase-filed simulation of non-isothermal solidification. Materials Today Communications, 2021, 28, 102712.	1.9	0
86	Selfâ€Assembled Epitaxial Ferroelectric Oxide Nanospring with Super calability (Adv. Mater. 13/2022). Advanced Materials, 2022, 34, .	21.0	0
87	Response to Comment on "Improper molecular ferroelectrics with simultaneous ultrahigh pyroelectricity and figures of merit― Science Advances, 2022, 8, .	10.3	Ο